Int. J. Heat Mass Transfer. Vol. 25, No. 3, pp. 409–418, 1982
Printed in Great Britain

0017-9310/82/030409-10 \$03.00/0

HEAT TRANSFER TO AIR FROM A YAWED CYLINDER

J. S. KRAABEL
Sandia National Laboratories, Livermore, CA 94550, U.S.A.
A. A. MCKILLOP and J. W. BAUGHN
University of California, Department of Mechanical Engineering, Davis, CA 95616, U.S.A.

(*Received* 29 *January* 1981 *and in revised form* 24 *July* 1981)

Abstract—An experimental program is reported on heat transfer to air from a yawed cylinder with a uniform temperature. The Independence Principle is confirmed for the laminar boundary layer region over the range of yaws investigated (20–60°). At high normal Reynolds numbers, Re_n, (based on the velocity component normal to the cylinder) and low yaws, the local normalized Nusselt numbers, $Nu_\theta/\sqrt{Re_n}$, in the wake region appears nearly independent of yaw and Re_n; whereas at low Re_n the local normalized Nusselt number is dependent upon both position and Re_n. The heat transfer results at high yaws show a marked difference from those at low yaws.

NOMENCLATURE

A,	area [m^2];
C_e,	epoxy conductance [mW/°C];
D,	diameter [m];
E,	voltage [V];
f,	shedding frequency of vortices [s^{-1}];
h,	heat transfer coefficient, $q''/(T_w - T_{aw})$ [W/m^2°C];
I,	electric current [A];
j,	exponent;
k,	thermal conductivity [W/m°C];
L,	length of cylinder [m];
Nu,	Nusselt number [hD/k];
q,	heat rate [W];
q'',	heat flux [W/m^2];
R_{lw},	lead wire resistance [Ω];
Re,	Reynolds number [$U_\infty D/\nu$];
Re_n,	normal Reynolds number [$DU_\infty \cos\beta/\nu$];
S,	Strouhal number [fD/U_∞];
T,	temperature [K];
T_{ac},	adiabatic cylinder temperature;
ΔT_m,	$= T_{\infty m} - T_{ac}$;
T_{aw},	adiabatic wall temperature;
$T_{\infty m}$,	measured free-stream temperature;
δT,	temperature variation;
T_s,	stagnation temperature;
T_{su},	sensor temperature with the sensor heater off;
T_w,	wall temperature;
U_∞,	freestream velocity [m/s];
x,	surface distance from stagnation point.

Greek symbols

β,	yaw;
ε,	total hemispherical emissivity;
θ,	circumferential angle [degrees];
μ,	viscosity [kg/m-s];
ν,	kinematic viscosity [m^2/s];
ρ,	air density [kg/m^3];
σ,	Stefan–Boltzmann constant, $= 5.6693 \times 10^{-8}$ W/m^{2}K^4.

Subscripts

c,	cylinder;
crit,	critical;
mht,	minimum heat transfer;
0,	stagnation point;
m,	mean;
r,	rear stagnation point or reference value;
rad,	radiation;
s,	sensor;
sep,	separation;
∞,	free-stream.

INTRODUCTION

THE FORCED convective heat transfer from a cylinder to air has been studied for both cross-flow and for yawed flow. Although the cross-flow phenomenon has been studied extensively, experimental values for the local and mean heat transfer coefficient for other than cross-flow are lacking. This investigation expands our knowledge of heat transfer from single cylinders in cross-flow to include other flow angles.

The research described in this paper is primarily experimental, based on local and mean heat transfer at two Reynolds numbers, 34,000 and 106,000, and yaws varied from cross-flow ($\beta = 0°$) to 60°. The surface of the cylinder was held at a constant temperature about 10°C greater than free-stream temperature, which assures nearly constant air properties. In order to approximate an infinite cylinder and yet minimize blockage, an aspect ratio ($L/D \cos\beta$) of 21 was chosen. This value yields a blockage of 8% for the tunnel used. Free-stream turbulence intensity was less than 0.4%.

FLOW PATTERNS

Cross-flow

A description of cross-flow over a circular cylinder has emerged from the work of several investigators [1–5]. These have shown that for subcritical flow ($10^3 \le Re \le 3 \times 10^5$) a laminar boundary layer exists in the region $0 \le \theta \le \theta_{sep}$ (see Fig. 1). The local free stream velocity accelerates from the stagnation line, thereby

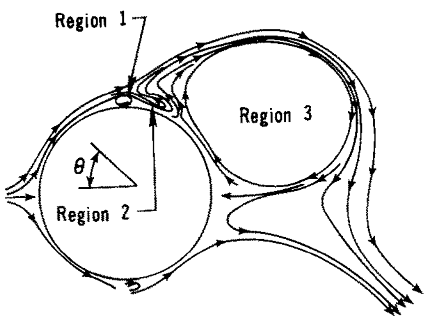

FIG. 1. Sketch of flow field (from [2]).

decreasing the pressure until it reaches approx. 65°, after which the flow decelerates and the boundary layer finally separates. The point of separation depends upon the Reynolds number; as Reynolds number increases, it moves forward toward the stagnation point until it reaches a minimum value of about $\theta_{sep} = 74°$ at $Re = 1.5 \times 10^5$ [1, 4, 5], thereafter, it shifts rearward until critical flow is reached [4, 5]. Coder's [5] data agree with the lower values of Achenbach's [4] in this Re region. Each found scatter in the values of θ_{sep}, but concluded that there was a continuous increase in θ_{sep}. In the laminar boundary layer region, analysis and experimentation are in good agreement.

Once separation occurs, three distinct regions appear for the Reynolds number range of 10^4–10^5, as shown in Fig. 1. The first of these develops immediately downstream of separation as a separation bubble. The resulting vortex formed is relatively stationary and produces a negative wall velocity gradient. A similar separation bubble develops on the opposite side of the cylinder. The second region results from the reattachment of the shear layer where the wall velocity gradient again becomes positive. The third region, further downstream, is characterized by a large periodic vortex which forms alternately on each side of the cylinder. This vortex, when fully formed, will contact the surface from 150° to 190° and will cause its own negative wall velocity gradient. Concurrently, the shear layer on the opposite side of the cylinder is in contact with the surface to $\theta \approx 150°$.

The onset of turbulence in the first two regions at subcritical flow has been examined by Bloor [3]. She has concluded that for Reynolds numbers greater than 30,000 the detached shear layer becomes turbulent in a transitional zone from 92 to 120°. Since reattachment occurs around 100° at this Reynolds number, the reattached shear layer is probably turbulent. Son and Hanratty [1] concluded that the size of the separation bubble approaches a minimum for $Re \geq 50{,}000$ and remains constant until Re_{crit}. For these Reynolds numbers, turbulence is sure at reattachment.

Bloor states that of prime importance in the development of turbulence is the onset of 3-dim. flow. Furthermore, she suggests (from the theory by Hama) that 3-dim. fluctuations (presumably a result of the oscillating nature of the wake) when imposed upon the gross flow structure can create the necessary 3-dim. flow. Son and Hanratty [1] hypothesize the same development of turbulent flow on the rear of the cylinder.

The oscillating of the wake in region three affects the flow throughout. The time-dependent study by Dwyer and McCrosky [6] and the mean flow measurements of Achenbach [4] in the boundary layer region show agreement in mean flow properties such as pressure distribution, free stream velocity, and wall shear stresses.

Finally, the Strouhal number, fD/U_∞, appears to decrease slightly for $5 \times 10^3 \leq Re \leq 4 \times 10^4$ and to remain constant thereafter until $Re = 10^5$. The flow patterns then appear to be independent of Re in the range of 5×10^4 to 10^5.

Yawed flow

A less complete description of yawed flow over a cylinder evolves from several reported studies [7–10]. A laminar boundary layer, once again, forms over the leading portion of the cylinder. In subcritical flow its properties are independent of the velocity along the cylinder (spanwise velocity), a phenomenon called "the Independence Principle" [8], and are characterized by the normal Reynolds number, Re_n. For low yaws at subcritical flow, the pressure distribution in the region before separation is the same as for cross-flow, a necessary requirement for the Independence Principle to hold. This independence breaks down, however, for high yaws ($\beta = 50°, 60°$). Bursnall and Loftin [9] have shown that for a yaw of 60° the pressure distribution in this region differs from that of cross-flow.

Over yawed cylinders, beyond the point of separation, spanwise velocity promotes an earlier transition to turbulent flow in the free shear layer [7, 10]. Thus, factors other than the cross-flow critical Reynolds number determine in part when the boundary layer becomes turbulent. Bursnall and Loftin, in fact, found that the Reynolds number for which the flow is critical varies little with yaws less than 30°. For a yaw of 60°, however, the critical number is 0.3 times the value for cross-flow. In a study at $Re = 20{,}000$, Smith *et al.* [7] demonstrated that transition to turbulence in the wake was induced sooner by increasing the yaw for a given Re_n; the size of the periodic vortex diminished when the yaw was increased; for large yaws ($\beta = 60°$) the initiation of transition appeared to have reached the boundary layer region; and the Strouhal number has the same constant value as for normal flow when defined in terms of the normal velocity component, fD/U_n. This last conclusion has also been shown to be true by Surry and Surry [11] who found $S = 0.19$ for $4 \times 10^3 < Re_n \leq 6.5 \times 10^4$.

Although the results of [7] are restricted to $Re_n < 2 \times 10^4$, their pressure drag coefficient appears to become independent of yaw for $Re_n > 2 \times 10^4$ and position for the onset of turbulence occurs at separation for $Re > 2 \times 10^4$ and $\beta \leq 30$.

HEAT TRANSFER

Cross-flow

The heat transfer characteristics in the laminar boundary layer have been investigated both analytically and experimentally. Frössling [12] solved the boundary layer equations by using a power series expansion employing the free-stream velocity expression of Hiemenz. His results were presented in terms of the dimensionless parameter $Nu_\theta/\sqrt{Re}$. Differences between his results and experiments [13, 14] can be attributed to such effects as free-stream turbulence, blockage, and non-constant wall temperatures.

All studies on heat transfer in the separated region have been experimental. This present investigation parallels the work of Schmidt and Wenner [13] and Achenbach [14] in that it involves the same Reynolds numbers and the same constant wall temperature, permitting comparison. As pointed out in the flow pattern section, there appear to be three distinct regions: a secondary vortex, a reattachment of the shear layer, and an oscillating main vortex. The reattachment, furthermore, may be laminar or turbulent depending upon whether or not transition has taken place in the separated shear flow. Heat transfer should reflect this type of reattachment flow.

Above $Re = 50{,}000$ the reattached flow must certainly be turbulent. In this case both Schmidt and Wenner [13] and Achenbach [14] show that the Frössling number reaches a minimum after flow separation and then steadily increases to the rear stagnation point. The curves have a local minimum slope around $\theta \approx 140°$, probably indicating the end of the reattachment region and final separation into the main vortex. The flow at this position should be oscillatory since the main vortex is oscillatory in nature.

At low Reynolds numbers ($5000 < Re < 25{,}000$) the Frössling number curve has two local minima: one around 85°, as in the case of high Re, and the other around 120–130° [13, 15]. This second minimum probably indicates a laminar reattachment. The data of Schmidt and Wenner are not consistent and show differences with different diameter cylinders at similar Re. In the range of Re between 30,000 and 40,000, some curves have only one minimum; others have two minima.

Several other points are worth noting from the studies of [13, 14]. As the Re increases, the point of first minimum heat transfer moves closer to the forward stagnation point; however, both studies indicate that this point occurs downstream of separation. Finally, for $\frac{1}{2}\,Re_{\mathrm{crit}} \le Re \le Re_{\mathrm{crit}}$, the Frössling number curves behave as though partial turbulent flow existed at separation: the point of minimum heat transfer moves downstream, as does the point of flow separation; a local maximum occurs just downstream of separation but, unlike fully turbulent flow, the maximum heat transfer still occurs at the rear stagnation point.

Yawed flow

Analytical results of heat transfer in the laminar boundary layer are the same as for cross-flow with U_∞ replaced by $U_\infty \cos\beta$. Experimental studies [16] have been confined to total heat transfer numbers and do not show a consistent relation between Nu_m and β.

EXPERIMENTAL APPARATUS

The cylinder, shown in Fig. 2, was designed to maintain a constant wall temperature under operating conditions. It consists of three parts: the center test section containing all the instrumentation with an internal electric heater, and two outside cylinders, each independently heated, which act as guards to assure minimal heat loss from ends of the center test section.

The center test section is a tube 60 cm long, 4.817 cm o.d., and 0.50 cm thick. It was itself fabricated in several sections, as shown in Fig. 2. The center portion, hereafter referred to as the thermal measurement section, is copper; it is 5.08 cm long. The key features of the thermal measurement section are a heat flux sensor which can independently measure the local heat flux while maintaining the isothermal wall condition, and thermocouples for wall temperature measurement around the cylinder.

The thickness of the wall and the high thermal conductivity of the copper are sufficient to assure that the surface temperature variation is small compared to the wall to free-stream temperature difference. An analysis presented in [17] shows the maximum variation in wall temperature should be

$$\frac{\delta T}{T_w - T_\infty} \le \pm\,0.009. \tag{1}$$

The experimental results showed a variation of this ratio of $\pm$ 0.006, or less than 1%.

The heat flux was measured with a sensor which was

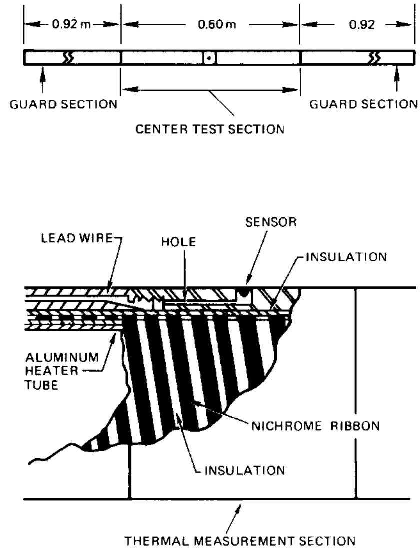

FIG. 2. Test cylinder with details of the thermal measurement section.

designed to obtain an accurate local heat flux measurement with minimal disturbance to either the flow or the isothermal wall condition. The details of the design and construction are given in [18]. An error analysis of the sensor shows an accuracy of $\pm$ 2% in the range of this experiment. The sensor heat transfer area on the surface of the cylinder is 14.30 mm^2; the sensor subtends an angle of 9.5°.

The wall temperature was measured with thermocouples which were installed 90, 180 and 270° circumferentially from the heat flux sensor and were calibrated in place. The accuracy of the temperature measurements was $\pm$ 0.1°C. Forty gauge Chromel–Constantan thermocouple wire was used to minimize conduction loss and to produce a high voltage output per degree of temperature difference.

The center test section was completed with the addition of two aluminum sections and two stainless steel spacers; all thermocouples were fed out through a longitudinal hole in the test section so as to maintain them at the wall temperature and thereby minimize temperature gradients. The test section was heated by nichrome ribbon spiralled around an insulated aluminum tube placed concentrically within the main tube.

Finally, two guard sections, independently heated in a similar manner to the test section, were added to each end. Differential thermocuples were installed across the spacer and between the center test sections. The power on the guard sections was adjusted to keep this differential temperature near zero, preventing end heat losses.

The cylinder was machined smooth and then polished with a chemical polish. It was then placed in a wind tunnel with a cross-section of 1.02 × 0.61 m and length 2.03 m. The blockage was 8%. Only the portion of the guard heaters within the tunnel was heated. A gunner's quadrant was used to measure the angle of rotation. The accuracy was estimated to be $\pm$ 0.1°. The wind tunnel is a low speed, low turbulence level ($Tu \leq 0.4\%$) tunnel with a uniform core velocity of better than 1%.

The free-stream temperature probe consisted of a calibrated thermocouple mounted within a ceramic insulating rod. The probe was located normal to the air flow. A pitot-static tube was used to measure free-stream velocity. A complete description of the experimental apparatus can be found in [17].

DATA REDUCTION

The experimental program was designed to determine the local heat transfer coefficient defined by

$$h_\theta = \frac{q''_\theta}{T_w - T_{aw}(\theta)} \tag{2}$$

as a function of yaw (β = 0, 20, 30, 40, 50 and 60°) and the Reynolds number (Re = 34,000 and 106,000). The local heat flux measured by the sensor is

$$q''_\theta = \frac{1}{A_s}[I_s E_s - I_s^2 R_{lw} - \varepsilon\sigma(T_w^4 - T_\infty^4)]. \tag{3}$$

The radiation correction is estimated to be about 0.2%.

The wall temperature, T_w, was measured directly and was found to be uniform within $\pm$ 0.06°C. $T_{aw}(\theta)$ is the local adiabatic wall temperature, that is, the local temperature that an insulated surface would attain. In the absence of compressibility effects, T_{aw} is the free-stream static air temperature. In our experiments, however, $T_s - T_\infty \leq 0.6$°C and cannot be neglected since $T_w - T_{aw} \approx 10$°C which could result in a 6% error in the heat transfer coefficient.

We determined T_{aw} as follows. An adiabatic temperature, T_{ac}, was defined as the mean temperature of the cylinder in the absence of any net heat transfer. Both T_{ac} and T_{aw} are functions of β and U_∞; T_{aw} is also a function of θ. Neither temperature was measured directly in this experiment. To obtain values of $T_{aw}(\theta)$ and T_{ac}, the following tests were run. The sensor and the cylinder, both unheated, were allowed to come to thermal equilibrium with the free-stream air. The temperature difference between the cylinder and the sensor, $T_{su} - T_{ac}$, and the difference between the average cylinder temperature and the free-stream probe temperature, $T_{\infty m} - T_{ac}$, were measured at each circumferential position. We defined

$$T_{\infty m} - T_{ac} = \Delta T_m(\beta, Re), \tag{4}$$

ΔT_m = 0.25°C for β = 0° and Re = 106,000, and decreased to 0 for β = 60°. ΔT_m was found to be zero for all β's at the lower Re.

With ΔT_m and $T_{su} - T_{ac}$ known, T_{aw} (θ) can be evaluated from an energy balance on the unheated sensor. Let C_e be the thermal conductance between the sensor and the cylinder. For our test assembly, C_e was found experimentally to be 11.55 mW/°C. Now

$$h_\theta A_s[T_{aw} - T_{su}] = C_e[T_{su} - T_{ac}].$$

With the aid of equation (4), we can write this equation as

$$T_{aw} = T_{\infty m} - \Delta T_m + (T_{su} - T_{ac})\left(1 + \frac{C_e}{h_\theta A_s}\right). \tag{5}$$

The cylinder temperature, T_w, was taken to be the average of the three wall measurements (this was within $\pm$ 0.02°C of the average).

Combining equations (2), (3) and (5), we obtain the expression for h_θ in terms of the measured quantities:

$$h_\theta = \frac{E_s I_s - I_s^2 R_{lw} - q_{rad_s} + (C_e + h_\theta A_s)(T_{su} - T_{ac})}{A_s(T_w - T_{\infty m} + \Delta T_m)}. \tag{6}$$

The value of h_θ is found by iteration. Since the value of $A_s h_\theta$ ($T_{su} - T_{ac}$) was never more than 1% of the numerator, only one iteration was necessary.

The mean heat transfer coefficient defined by

$$h_m = \frac{q_c}{A_c(T_w - T_{ac})} = \frac{E_c I_c - I_c^2 R_{lw} - q_{rad}}{A_c(T_w - T_{\infty m} + \Delta T_m)} \tag{7}$$

was found to agree closely with the integrated value given by

$$h_m = \frac{1}{\pi}\int_0^{\pi} h_\theta d\theta \tag{8}$$

RESULTS

Data were collected at Reynolds numbers of 34,000 and 106,000 for yaws of 0, 20, 30, 40 and 50°, and for 60° at the higher *Re*. The results are displayed and discussed in terms of a modified Frössling number, $Nu_\theta/\sqrt{Re_n}$. Since $\mu^{1/2}/k\rho^{1/2}$ is only slightly dependent upon temperature for air, ambient temperature was used.

Cross-flow

Figure 3 shows our experimental results. The curves are the applicable results of [13, 14]. We performed a finite difference solution of the laminar boundary equations [17] for Reynolds numbers of 18,000 and 170,000; the free-stream velocity data of Hiemenz [19] and Eckert [20], respectively, were used. Our analytical boundary layer solution is indistinguishable from our experimental results in this region. The laminar boundary layer data were reproducible with a standard deviation of less than 1%. The data in the wake were equally reproducible for a given positioning of the cylinder; however, if the cylinder had been moved to a different yaw and then returned, the standard deviation could increase to between 2 and 5%. Finally, symmetry between top and bottom of the cylinder was within ± 2%.

The difference between our experimental results and those of [13, 14] are most likely due to differences in free-stream turbulence, in blockage, and to non-constant circumferential temperature distribution. In discussing the results of Schmidt and Wenner [13], Schlichting [21] stated that the increasing free-stream turbulence level produced by increasing the Reynolds number accounted for the discrepancy between theory (Frössling [12]) and experiment. At the higher Reynolds number, therefore, the differences can be explained, in part, by the enhancement of heat transfer due to turbulence. In Achenbach's [14] results, the point of minimum heat transfer is farther downstream and the Frössling numbers are higher at both stagnation points. Both effects may be attributed to a slightly higher blockage and a variation in the wall temperature distribution.

Yawed flow

As a result of the Independence Principle, the modified Frössling number, $Nu_\theta/\sqrt{Re_n}$ should be the same for all yaws in the laminar boundary layer region. The results presented in Fig. 4 and 5 show that such is the case, except for the higher values of $\beta = 50°$ and $\beta = 60°$ near separation. Regardless of Re_n and β, the mean value of $Nu_0/\sqrt{Re_n}$ is 0.955 with a standard deviation of ± 0.7%. Our analytical value is 0.954.

The Frössling numbers on the rear of the cylinder for $Re = 106{,}000$ and for $\beta \leq 40°$ appear to coincide. The standard deviation of each data point on the rear of the cylinder is about 2%.

The low Reynolds number data exhibit different behaviour in the wake region. $Nu_\theta/\sqrt{Re_n}$ decreases as the yaw is increased to 30°, but is the same for 40°.

The results for the high yaws ($\beta \leq 50°$) for both *Re* show a different distribution. The delayed minimum heat transfer is followed by a region of rapidly increasing heat transfer where $Nu_\theta/\sqrt{Re_n}$ becomes larger than for the cross-flow case. The 50° data are non-symmetric with the rear stagnation point located at 170° for the low *Re*, and at 185° (data point not shown) for the high *Re*.

The effect of yaw on the region of minimum heat transfer, as specified by $Nu_\theta/\sqrt{Re_n}$, is to both broaden and move it rearward, as is shown for each Reynolds number in Fig. 6. The actual point of minimum heat

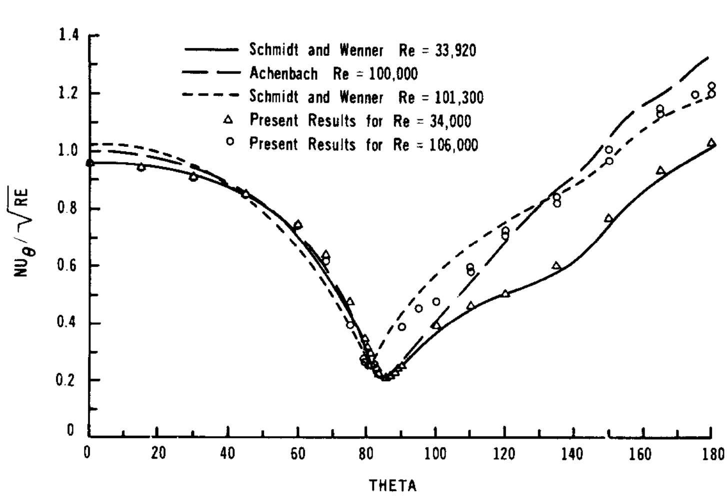

FIG. 3. Comparison of cross-flow results ($Re = 106{,}000$ and 34,000).

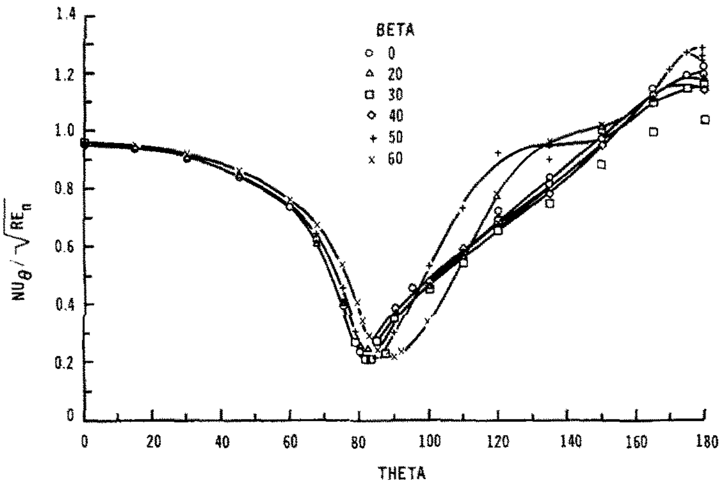

Fig. 4. Normalized Nusselt number results for yawed flow (Re = 106,000).

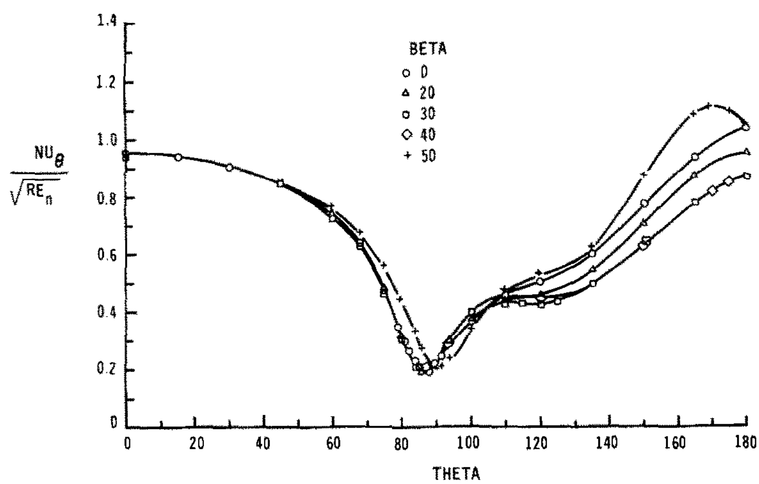

Fig. 5. Normalized Nusselt number results for yawed flow (Re = 34,000).

transfer moves further rearward with increasing yaw and is plotted versus Re_n in Fig. 7. These angles were estimated from Fig. 6. It should be noted that these results are affected, in magnitude and probably in the location of the minimum, by the finite sensor size.

The mean values of the Nu are shown in Fig. 8. Excellent agreement was found between values evaluated from equations (7) and (8).

DISCUSSION

Cross-flow

The point of minimum heat transfer does not coincide with the point of separation; it moves forward with increasing Re in conjuction with the movement of the point of separation. The change in slope of the Frössling number curve near $\theta = 95°$ at $Re = 10^5$ apparently marks the end of the effect of the separation bubble region; at the lower Re, this change in slope is noticeable at $\theta \approx 100°$. The shapes of the Frössling number curve in the reattachment region, moreover, indicate turbulent reattachment, as expected at the given Reynolds numbers.

Low yawed flow ($\beta \leq 40°$)

The applicability of the Independence Principle for laminar boundary layer heat transfer has been established for $\beta \leq 40°$. A surprising result, however, is the near coincidence of the modified Frossling number in the wake region at the higher Re. The flow is 3-dim. and probably turbulent from the point of separation, and there is no *a priori* reason why the yaw should not influence the character of the 3-dim. flow. However, since the Strouhal number is the same for all yaws when based on the normal velocity, and since position of the onset of turbulence apparently becomes independent of Re_n for low yaws, perhaps the above result

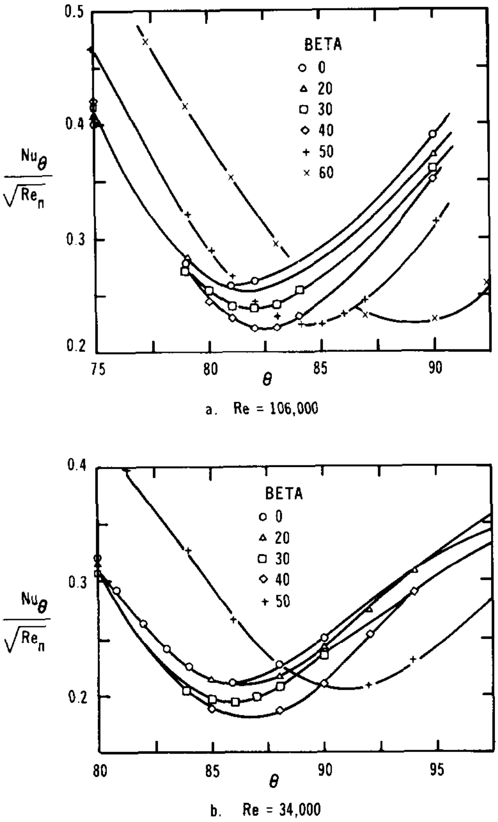

FIG. 6. Normalized Nusselt number in the minimum heat transfer region.

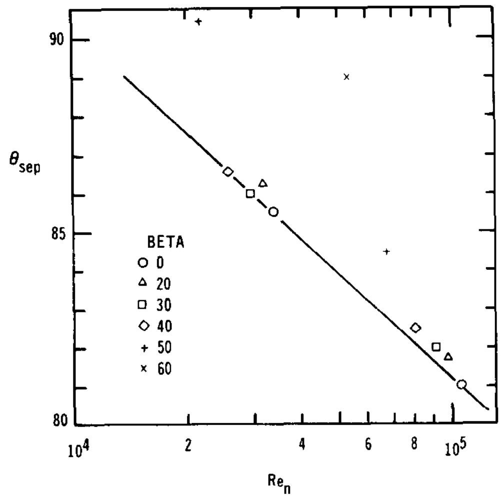

FIG. 7. Position of minimum heat transfer as a function of Re_n.

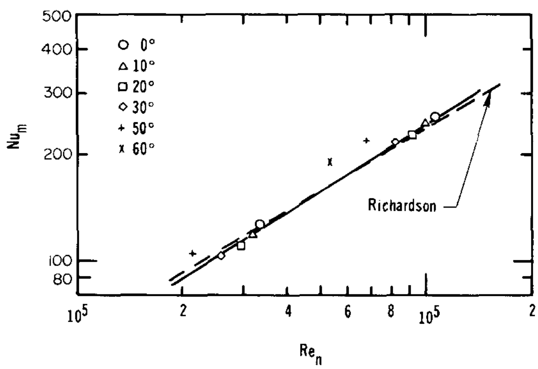

FIG. 8. Mean Nusselt number for different yaws.

should have been anticipated. In cross-flow, for $Re > 50{,}000$, the flow patterns remain quantitatively the same, including three-dimensionality. If the yaw does not affect the flow at low yaw then we might anticipate the flow patterns, and hence the heat transfer might be nearly the same if $50{,}000 \leq Re_n \leq 100{,}000$. Such is the case for the higher *Re*.

Such is not the case, however, at the lower *Re*. Even in cross-flow the flow patterns are *Re*-dependent for $Re < 50{,}000$, and therefore the heat transfer numbers should differ for each Reynolds number. Schmidt and Wenner [13], in fact, do show that in the wake the Frössling number decreases with decreasing *Re*. For low yaws, we find a like dependency of the modified Frössling number upon Re_n. To facilitate the prediction of heat transfer in this latter case, we looked at the possibility that $Nu_\theta/\sqrt{Re_n}$ is a function of θ and Re_n only, that is, nearly independent of β. In Fig. 9, we test this idea by comparing the data of [13] at Reynolds numbers of 33,920 and 21,200 with our results for yawed flow, $26{,}000 \leq Re_n \leq 33{,}600$. Reasonable agreement is found.

The rear stagnation point heat transfer has been much investigated in crossflow where data have been correlated in terms of $Nu_{180} = aRe^b$. The results from the present investigation, for $\beta \leq 40^\circ$ are shown in Fig. 10. The value of $b = 0.67$ compares favorably with those of Richardson's 2/3 [22] and Seban and Levy's 0.66 [23]. More work is necessary, however, before such correlations can be recommended for general use.

High yawed flow

The heat transfer data for yaws of 50 and 60° indicate a change of flow patterns. Thus, the point of minimum heat transfer shifts rearward; the modified Frössling number in the rear stagnation region nearly coincides with the cross-flow number; and the modified Frössling number, before boundary layer separation, obtains higher values due, in part, to the influence of the change in pressure distribution as critical flow is approached. These results, in fact, show similar patterns to the results of [13, 14] in cross-flow for $\frac{1}{2} Re_{crit} < Re < Re_{crit}$. In addition, Bursnall and Loftin [9] have shown that, for $\beta = 60^\circ$, critical flow occurs at $Re_n = 10^5$. For yaws of 50 and 60°, our values of Re_n are 68,135 and 53,000, respectively, falling in the range $\frac{1}{2} Re_{crit} \leq Re_n \leq Re_{crit}$. The fact that higher heat transfer

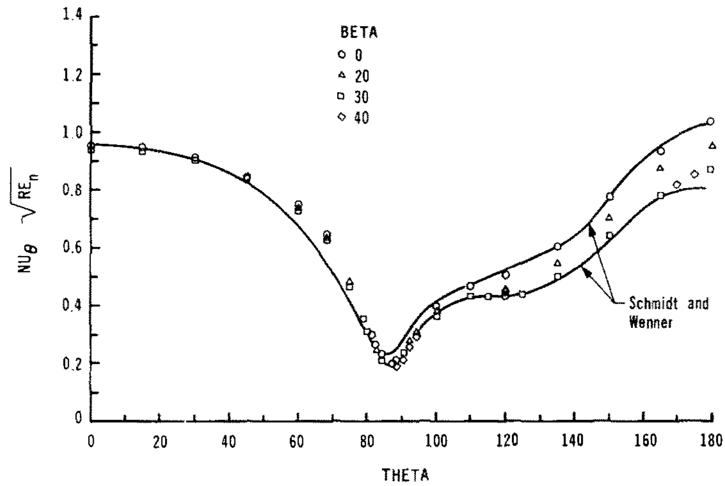

FIG. 9. Comparison of low yaw angle data with Schmidt and Wenner [13] (Re = 33,920 and 21,200).

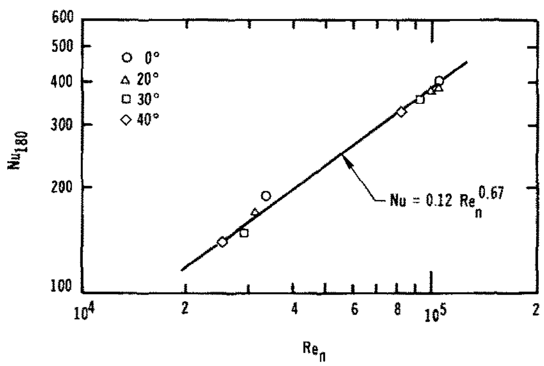

FIG. 10. Rear stagnation Nusselt number for low yaws.

occurs at 50° rather than 60° would be consistent with this idea since Re_n decreases with increased yaw. Further study is needed on the fluid dynamics of separated flow at high yaws and, in particular, how the flow in the separated region encroaches on the unseparated boundary layer. While the results for β = 50° and Re = 34,000 show some characteristics of the approach of critical flow, it would be wrong to assume such to be the case. The asymmetry in heat transfer at 180° for the 50° yaw at both Reynolds numbers signifies a complex flow pattern that cannot be explained in terms of proposed models of flow patterns around cylinders.

Mean heat transfer

Although we have shown that there should be at least three regions which determine the mean heat transfer number, several workers have chosen to correlate data in the following form.

$$Nu_m = C_1 Re_n^{1/2} + C_2 Re_n^j. \tag{9}$$

For $\beta \leq 40°$, C_1 was taken to be 0.361 and C_2 and j were determined to be 0.023 and 0.75, respectively, by a least squares fit. Equation (9), together with the Nu_m data, is shown in Fig. 8. Richardson's equation is also shown.

The Nu_m for cross-flow are within 5% of the values predicted by the correlation equation (10) of Churchill and Berstein [24]. For the 8% blockage of this experimental program, the correction suggested by Morgan [16] would amount to a change in the Re of 4% and a corresponding change in Nu_m of only 2%.

Another way to look at the effect of yaw on total heat transfer is to examine the ratio of heat transferred from the rear portion of the cylinder to the total heat transfer. This ratio is plotted in Fig. 11 vs Re_n; the data of [13] are also included. Once again for $\beta \leq 40°$, the ratio is nearly independent of β. Figure 11 shows that for $Re > 1.2 \times 10^5$ the ratio is leveling off at a value of 0.55 for normal flow. For $\beta \geq 60°$ this is the same value for yawed flow for $Re_n > 5 \times 10^4$, the region denoted as $\frac{1}{2} Re_{crit} \leq Re_n \leq Re_{crit}$. One can imagine, when the low Re_n point is included, that the effect of yawing is to shift the curve to the left.

CONCLUSIONS

In summary, four conclusion are drawn from the results of this investigation:

(1). The Independence Principle is valid for heat transfer at the stagnation line and in the laminar boundary layer.

(2). Although the Independence Principle would not be expected to extend to the wake, it is observed that the local heat transfer to the wake is not greatly affected by yaw for $\beta \leq 40°$.

(3). The heat transfer results can be explained in terms of a secondary vortex which is located downstream of an initial separation point and is followed by a primary eddy.

(4). For high yaws and high Re_n, the heat transfer data are similar in some ways to that which occurs for cross flow data approaching critical flow.

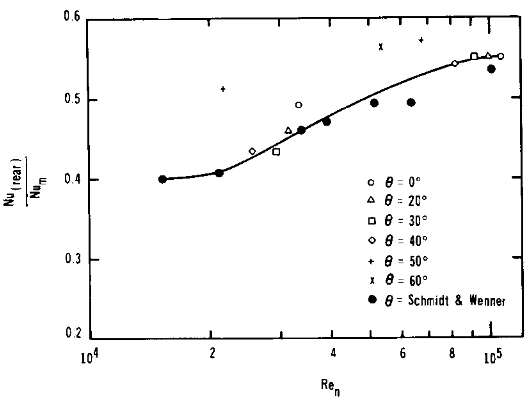

FIG. 11. Portion of heat transfer in the rear region.

Acknowledgements—This research was supported under NSF Grant 75–19046.

REFERENCES

1. J. S. Son and T. J. Hanratty, Velocity gradients at the wall for flow around a cylinder at Reynolds numbers from 5×10^3 to 10^5, *J. Fluid Mech.* **35**, 363 (1969).
2. M. Lebouche and M. Martin, Convection forcée autour du cylindre; sensbilité aux pulsations de l'écoulement externe, *Int. J. Heat Mass Transfer* **18**, 1161 (1975).
3. M. S. Bloor, The transition to turbulence in the wake of a circular cylinder, *J. Fluid Mech.* **19**, 290 (1964).
4. E. Achenbach, Distribution of local pressure and skin friction around a circular cylinder in cross-flow up to $Re = 5 \times 10^6$, *J. Fluid Mech.* **34**, 625 (1968).
5. D. W. Coder, Location of separation on a circular cylinder in crossflow as a function of Reynolds number, NSRDC Report 3647, AD 7333983, Nov., 1971.
6. H. A. Dwyer, and W. J. McCroskey, Oscillating flow over a cylinder at large Reynolds number, *J. Fluid Mech.* **61**, 753 (1973).
7. R. A. Smith, W. T. Moon and T. W. Kao, Experiments on the flow about a yawed circular cylinder, *J. Basic Engng* **94D**, 771 (1972); Institute of Ocean Sciences and Engineering Report 70-7, Dec. 1970, Catholic University of America, AD 725136.
8. W. W. Chiu and J. H. Lienhard, On real fluid over yawed circular cylinders, *J. Basic Engng* **89D**, 851 (1967).
9. W. J. Bursnall and L. K. Loftin, Jr., Experimental investigation of the pressure distribution about a yawed circular cylinder in the critical Reynolds number range, NACA TN 2463 (1951).
10. S. E. Ramberg, The influence of yaw angle upon the vortex wakes of stationary and vibrating cylinders, NRL-MR-3822 (1978).
11. J. Surry and D. Surry, The effect of inclination on the Strouhal number and other wake properties of circular cylinders at subcritical Reynolds numbers, UTIAS Tech. Note 116, AD 65779 (Aug. 1967).
12. N. Frössling, Evaporation, heat transfer and velocity distribution in two-dimensional and rotationally symmetrical laminar boundary layer, NACA TM 1432 (1958).
13. E. Schmidt and K. Wenner, Heat transfer over the circumference of a heated cylinder in transverse flow, NACA TM 1050 (1943).
14. E. Achenbach, Total and local heat transfer from a smooth circular cylinder in cross-flow at high Reynolds number, *Int. J. Heat and Mass Transfer* **18**, 1387 (1975).
15. M. I. Boulos and D. C. T. Pei, Dynamics of heat transfer from cylinders in a turbulent air stream, *Int. J. Heat Mass Transfer* **17**, 767 (1974).
16. V. T. Morgan, The overall convective heat transfer from smooth circular cylinders, *Advances in Heat Transfer*, Vol. 11, p. 199. Academic Press, New York (1975).
17. J. S. Kraabel, Heat transfer to air from a yawed isothermal cylinder, Ph.D. Thesis, University of California (1979).
18. J. S. Kraabel, J. W. Baughn and A. A. McKillop An instrument for the measurement of heat flux from a surface with uniform temperature, *J. Heat Transfer* **102**, 576 (1980).
19. K. Hiemenz, Die Grenzschicht an einem in den gleichformigen Flussigkeitsstrom eingetauchten geraden Kreiszylinder. Thesis, Göttingen (1911) see also Frössling or Schlichting.
20. E. R. G. Eckert, Die Berechnung des Warmeuberganges in der laminaren Grenzschicht umströmter Körper, *Forschungsh* **416B** (1942).
21. H. Schlichting, *Boundary Layer Theory*, 6th edn. McGraw-Hill (1968).
22. P. D. Richardson, Heat and mass transfer in turbulent separated flows, *Chem. Engng Sci.* **18**, 149 (1963).
23. R. A. Seban and A. M. Levy, The effect of a downstream splitter plate on the heat transfer from a circular cylinder normal to an air stream, WADC TR 57–479 ASTITA AD 155765 (1957).
24. S. W. Churchill and M. Bernstein A correlating equation for forced convection from gases and liquids to a circular cylinder in crossflow, *J. Heat Transfer* **99**, 300 (1977).

TRANSFERT THERMIQUE AUTOUR D'UN CYLINDRE EN DERAPAGE

Résumé—On rapporte une étude expérimentale sur le transfert thermique autour d'un cylindre chauffé à température constante et en dérapage dans l'air. Le principe d'indépendance est confirmé pour la région de couche limite laminaire dans le domaine d'angle de dérapage étudié (20° à 60°). Aux grands nombres de Reynolds normaux Re_n (basés sur la composante normale de vitesse) et aux faibles angles, le nombre de Nusselt local et normalisé $Nu_\theta/\sqrt{Re_n}$ est dans la région de sillage, à peu près indépendant de Re_n et de l'angle; par contre, aux faibles Re_n le nombre de Nusselt local et normalisé dépend à la fois de la position et de Re_n. Les résultats du transfert thermique aux forts dérapages montrent une différence marquée avec ceux relatifs aux faibles dérapages.

WÄRMEÜBERGANG ZWISCHEN LUFT UND EINEM SCHRÄG ANGESTELLTEN ZYLINDER

Zusammenfassung—Es wird über experimentelle Untersuchungen zur Bestimmung des Wärmeübergangs zwischen Luft und einem schräg angestellten Zylinder mit gleichförmiger Temperatur berichtet. Für das Gebiet der laminaren Grenzschicht wird im Bereich der untersuchten Anstellwinkel zwischen 20 und 60° prinzipielle Unabhängigkeit bestätigt. Für große Reynolds-Zahlen Re_n (bezogen auf die Geschwindigkeitskomponente normal zum Zylinder) und kleine Anstellwinkel ist die lokale normierte Nusselt-Zahl $Nu_\theta/\sqrt{Re_n}$ im Nachlaufgebiet nahezu unabhängig von der Anstellung und von Re_n, während für kleine Reynolds-Zahlen die lokale normierte Nusselt-Zahl vom Ort und von Re_n abhängig ist. Die Wärmeübergangszahlen bei großen und kleinen Anstellwinkeln unterscheiden sich erheblich.

ТЕПЛОПЕРЕНОС ОТ НАКЛОННОГО ЦИЛИНДРА К ВОЗДУХУ

Аннотация — Проведено экспериментальное исследование переноса тепла к воздуху от равномерно нагреваемого наклонного цилиндра. Подтверждена справедливость принципа независимости для области ламинарного пограничного слоя в диапазоне углов наклона цилиндра от 20 до 60°. При больших значениях числа Рейнольдса Re_n, построенного по нормальной к цилиндру скорости, и малых углах наклона локальные нормированные значения числа Нуссельта $Nu_\theta/\sqrt{Re_n}$ в области следа не зависят от угла наклона и числа Re_n, в то время как при малых числах Re_n локальные нормированные значения числа Нуссельта зависят как от положения цилиндра, так и числа Re_n. Результаты по теплообмену при больших углах наклона значительно отличаются от данных, полученных при небольших углах.